PHYSICAL REVIEW B **95**, 205402 (2017)

# Effect of interactions on quantum-limited detectors

Gleb Skorobagatko,[1] Anton Bruch,[1] Silvia Viola Kusminskiy,[1,2] and Alessandro Romito[1,3]

[1] *Dahlem Center for Complex Quantum Systems and Fachbereich Physik, Freie Universität Berlin, 14195 Berlin, Germany*

[2] *Institute for Theoretical Physics, University Erlangen–Nürnberg, Staudtstraße 7, 91058 Erlangen, Germany*

[3] *Department of Physics, Lancaster University, Lancaster LA1 4YB, United Kingdom*

(Received 27 September 2016; revised manuscript received 7 February 2017; published 1 May 2017)

We consider the effect of electron-electron interactions on a voltage biased quantum point contact in the tunneling regime used as a detector of a nearby qubit. We model the leads of the quantum point contact as Luttinger liquids, incorporate the effects of finite temperature and analyze the detection-induced decoherence rate and the detector efficiency, $Q$. We find that interactions generically reduce the induced decoherence along with the detector's efficiency, and strongly affect the relative strength of the decoherence induced by tunneling and that induced by interactions with the local density. With increasing interaction strength, the regime of quantum-limited detection ($Q \to 1$) is shifted to increasingly lower temperatures or higher bias voltages respectively. For small to moderate interaction strengths, $Q$ is a monotonously decreasing function of temperature as in the noninteracting case. Surprisingly, for sufficiently strong interactions we identify an intermediate temperature regime where the efficiency of the detector increases with rising temperature.

DOI: 10.1103/PhysRevB.95.205402

## I. INTRODUCTION

Detecting the state of a quantum system is an invasive process, which necessarily modifies the system itself. In a continuous measurement description, the information on the system's state is gradually encoded in a classical (macroscopic) signal of a detector, which at the same time induces a modification of the state of the system [1,2]. In the simplest case of measuring an observable $A$ of a two-level system, where the detector distinguishes the two eigenstates of $A$, the process is characterized by a measurement time, $\tau_M$, after which the detector's signals for the different eigenstates can be resolved from the detector's noise. From the system's point of view, the detector backaction corresponds to a stochastic component of the state evolution, which asymptotically drives the system toward one of the measured eigenstates. On average, this backaction is quantified by the detector-induced decoherence time, $\tau_{\mathrm{dech}}$, after which the system is in an incoherent mixture of eigenstates of $A$. The fundamental disturbance associated with measurement in quantum mechanics is quantified by the fact that $\tau_{\mathrm{dech}} \leqslant \tau_M$. When the decoherence rate coincides with the rate of acquisition of information, backaction is minimal, which is referred to as quantum-limited detection. This continuous description of a quantum measurement is in fact appropriate for current readout methods of a variety of qubits and quantum devices [3–6].

The significance of quantum-limited detection is apparent in single shot measurements, as opposed to averaged measurement results. In a single shot measurement a quantum-limited detector induces a stochastic evolution of the system without any decoherence, and therefore a pure state remains as such during the measurement [2,7,8]; decoherence appears only as a result of averaging over the detector's outcome. This observation is at the basis of a number of techniques for quantum device control [2,9,10], precision measurement [11–13], and quantum information processing [14–17]. The experimental implementation of these techniques besides quantum optics [2] has been initiated in superconducting qubits where feedback loops [18] and single trajectory mapping [19] have been reported. Quantum-limited detection is therefore of interest in solid-state systems at large, where spin, charge, and topologically protected degrees of freedom are exploited for new quantum devices. A number of different detection schemes exist in these contexts. For example, charge sensors based on transport through semiconductor devices, such as quantum point contacts (QPCs), are used and proposed as sensors for, e.g., charge [6,20–26], spin [27,28], and topologically protected qubits [29].

Motivated by the evolution of the measurement process in solid-state systems, we analyze here the effect of interactions on quantum measurement, focusing on the detector's efficiency. Electron-electron interactions are generally important in solid-state systems. Specifically, we consider a charge qubit sensed by a nearby quantum point contact in the tunneling regime, which directly models charge sensing in experiments, and it can emerge as an effective description of certain detection schemes of superconducting qubits [30]. We consider two effects of the electrostatic coupling of the QPC to the charge state of the qubit: (i) a state-dependent tunneling term and (ii) a state-dependent coupling to the local density [31]. In the absence of interactions, the QPC is a quantum-limited detector for sufficiently low temperature. Both thermal fluctuations and local density couplings drive the detector away from its quantum limit working point [7,31–33]. We find that repulsive electron-electron interactions generically reduce both the rates of induced decoherence and of acquisition of information with respect to their noninteracting counterpart, although in different amounts. This difference is due purely to the local density interaction term, which contributes to decoherence but does not participate in the current and hence provides no information on the system's state. For increasingly strong interactions, the renormalization of the rates leads to the need for lower temperatures in order to reach the quantum limit of detection. In this case, interactions provide us with a slower detector. Remarkably, for sufficiently strong interactions we find an intermediate temperature regime where, as opposed to the noninteracting case, the measurement efficiency improves with increasing temperature.

 

The paper is organized as follows. In Sec. II we define the model and present the Hamiltonian of the system in the Luttinger formalism. Sections III and IV are devoted to calculating the rates of decoherence and acquisition of information, respectively. The decoherence rate is obtained by considering the reduced density matrix of the charge qubit in the presence of the QPC. We show that the two coupling mechanisms to the environment are separable and calculate the tunneling contribution via a cumulant expansion. The rate of acquisition of information is obtained by considering the full counting statistics of the problem. The effects of electronic interactions on the detection efficiency of the QPC are analyzed in Sec. V. The conclusions are presented in Sec. VI. Lengthy calculations have been relegated to the Appendixes.

## II. MODEL

We consider a double quantum dot (DQD) that realizes a charge qubit, in proximity of a QPC. The QPC is formed by a tunneling barrier between two semi-infinite one-dimensional (1D) quantum wires consisting of spinless interacting electrons, as depicted in Fig. 1. We treat the wires as Luttinger liquids.

The charge configuration of the DQD affects the tunneling of electrons at the QPC between right ($R$) and left ($L$) Luttinger liquids. Hence the current through the QPC acts as a charge detector of the double quantum dot. The total Hamiltonian of our problem consists of three terms,

$$H_\Sigma = H_{\mathrm{LL}} + H_{\mathrm{QD}} + H_{\mathrm{int}}, \tag{1}$$

where $H_{\mathrm{LL}}$ represents the Hamiltonian of both left and right Luttinger liquids, $H_{\mathrm{QD}}$ that of the DQD, and $H_{\mathrm{int}}$ denotes the interaction between the two. If we consider the QPC to be located at $x = 0$,

$$H_{\mathrm{LL}} = \frac{1}{2\pi}\sum_{j=L,R} v_g \int_{-\infty}^{0} \left\{ g(\partial_x\varphi_j)^2 + \frac{1}{g}(\partial_x\theta_j)^2 \right\} dx, \tag{2}$$

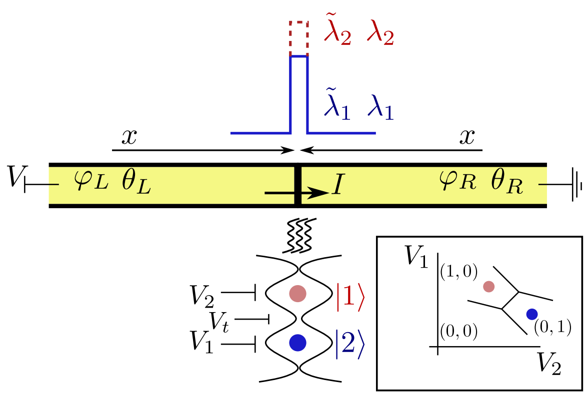


FIG. 1. Sketch of the system under consideration. A double quantum dot is capacitively coupled (wavy lines) to a tunnel junction between two Luttinger liquids. Two charge configurations, $|1\rangle$ (blue solid) and $|2\rangle$ (red shady), for an electron shared between the two dots induce different tunnel barriers, hence different currents, through the junction. The electron in the double dot can generically be in a coherent superposition of these two states, as controlled by external gate voltages, as sketched in the inset.

where $\theta_{L(R)}$ and $\varphi_{L(R)}$ are the usual charge and phase fields in the bosonic representation of the Luttinger liquid on the left (right) side of the QPC, $g$ is the dimensionless interaction parameter (which for repulsive interactions fulfills $0 < g \leqslant 1$, where $g = 1$ is the noninteracting limit) and $v_g$ is the group velocity of collective plasmonic excitations. We have chosen the coordinate systems on both left and right such that $x$ increases from $-\infty$ to zero, where the QPC is located. We have also set $\hbar = 1$, which holds hereafter along with $k_B = 1$.

The Hamiltonian of the DQD is

$$H_{\mathrm{QD}} = \sum_{n=1,2} \varepsilon_n c_n^\dagger c_n + \gamma(c_1^\dagger c_2 + c_2^\dagger c_1), \tag{3}$$

where $c_n^\dagger(c_n)$ are fermionic operators of creation (destruction) of an electron in the $n$th quantum dot ($n = 1,2$), $\varepsilon_n$ are the electronic level energies (with respect to the Fermi energy of an external electronic reservoir, which is chosen to be equal to zero), and $\gamma$ is the tunneling amplitude between the dot's levels. In the following, we assume that the DQD is, besides the nearby QPC, isolated from the electronic environment, with a total extra electron shared between the two dots. In this case, only the energy difference $\varepsilon_2 - \varepsilon_1 = \varepsilon$ is physical.

We define further the fields $\theta_\pm = 1/2[\theta_L \pm \theta_R]$ and $\varphi_\pm = 1/2[\varphi_L \pm \varphi_R]$, and we model the interaction term as (cf. Appendix A)

$$H_{\mathrm{int}} = \sum_{n=1,2} [a_0\lambda_n\partial_x\theta_+ + \tilde{\lambda}_n \cos(2\varphi_- + eVt)]|_{x=0} c_n^\dagger c_n, \tag{4}$$

where $\lambda_n$ represents the electrostatic coupling between the quantum dot and the Luttinger liquid leads at $x = 0$, and $\tilde{\lambda}_n$ characterizes the tunneling at the QPC. Both quantities are assumed to be real and positive, and they depend on the state of the DQD, $n$. The parameter $a_0$ is the short-distance cutoff that goes to zero in the continuum limit. This provides a high-energy cutoff to the model, $\Lambda_g = v_g/a_0$. Therefore, in our further analysis all energies fulfill $E \ll \Lambda_g$ and all times $t \gg 1/\Lambda_g$. $V$ is an externally applied voltage bias between left and right Luttinger liquids. In the limit of weak tunneling in which we are concerned here, this potential difference can be described by a local voltage drop at the QPC site [34,35]. In what follows, we denote the fields evaluated at $x = 0$ by simply omitting the spatial argument.

Note that in the choice of the interaction Hamiltonian, we have implicitly identified the states $|1\rangle \equiv c_1^\dagger|0\rangle$ and $|2\rangle \equiv c_2^\dagger|0\rangle$ as the charge eigenstates of the measurement device. The detector signal for these two states and the induced decoherence on their coherent superposition characterize the tunnel-coupled Luttinger liquids as a detector.

## III. DECOHERENCE

In this section, we calculate the decoherence rate caused by the tunnel-coupled Luttinger liquids on the DQD. To do so, we assume that at $t = 0$ the DQD is initialized in a coherent state $|\phi_0\rangle = \alpha|1\rangle + \beta|2\rangle$ and is decoupled from the detector (i.e., $H_{\mathrm{int}} = 0$). The state of the detector is determined by the Hamiltonian $H_{\mathrm{LL}}$ in Eq. (2) and by the temperature $T$ and applied voltage bias $V$. For $t > 0$, the coupling $H_{\mathrm{int}}$ is suddenly switched on and the evolution is determined by the

DQD interaction with the QPC. Importantly, we assume a vanishing interdot tunneling $\gamma = 0$ in Eq. (3) since we are interested in the pure decoherence induced by the detector (without relaxation processes). Let us note that physically $\gamma \neq 0$ is needed to create the initial coherent superposition $|\phi_0\rangle$, and $\gamma$ can be consistently assumed arbitrarily small so that the effect of the interdot tunneling is negligible throughout the relevant time scales of system-detector interactions ($t \ll 1/\gamma$). Alternatively, assuming total control of the experimental setup [22,23], $\gamma$ can be set to zero after preparing the coherent state.

To quantify the measurement-induced decoherence, we analyze the DQD reduced density matrix $\rho$, where the degrees of freedom of the environment (in this case, the LL) have been traced out. The initial density matrix $\rho(0) = |\phi_0\rangle\langle\phi_0|$ at $t = 0$ evolves at time $t$ to $\rho_{mn}(t) = e^{-i(\varepsilon_m-\varepsilon_n)t}\rho_{mn}(0)\langle U_n^\dagger(t)U_m(t)\rangle$, where $m,n = 1,2$, $H_{\rm QD}|n\rangle = \varepsilon_n|n\rangle$, $U_n(t) = \mathcal{T}_t \exp\{-i\int_0^t d\tau\, \mathcal{H}_{\rm int}^{(n)}(\tau)\}$, and $\langle\cdots\rangle$ denotes the quantum-statistical average over $H_{\rm LL}$ at temperature $T$. $\mathcal{T}_t$ ($\overline{\mathcal{T}}_t$) denote time- (anti-time-) ordering operators, and $\mathcal{H}_{\rm int}^n(s) = \langle n|\mathcal{H}_{\rm int}(s)|n\rangle$, where $\mathcal{H}_{\rm int}$ corresponds to $H_{\rm int}$ written in the interaction representation with respect to $H_{\rm LL}$. By using the equation of motion for the bosonic fields, it can be shown that $\mathcal{H}_{\rm int}^n$ in Eq. (4) can be written in terms of phase fields only (see Appendix A),

$$\mathcal{H}_{\rm int}^n(t) = -g\frac{\lambda_n}{\Lambda_g}\dot{\varphi}_+(t) + \tilde{\lambda}_n \cos[2\varphi_-(t) + eVt]. \tag{5}$$

To calculate the time evolution of the reduced density matrix, we first note that the fields $\varphi_+$ and $\varphi_-$ commute at equal times, $[\varphi_+(t),\varphi_-(t)] = 0$, which allows us in the following to evaluate their vacuum expectation values separately. We obtain

$$\rho_{mn}(t) = \rho_{nm}^*(t) = e^{-i(\epsilon_m-\epsilon_n)t}\rho_{mn}(0)Z_{mn}(t)\tilde{Z}_{mn}(t) \tag{6}$$

with

$$Z_{mn} = \left\langle e^{i\frac{g(\lambda_n-\lambda_m)[\varphi_+(t)-\varphi_+(0)]}{v_g}}\right\rangle, \tag{7}$$

$$\tilde{Z}_{mn} = \langle \mathcal{U}_n(t,0)^{-1}\mathcal{U}_m(t,0)\rangle, \tag{8}$$

with $\mathcal{U}_m(t,0) = \mathcal{T}_t e^{-i\tilde{\lambda}_m\int_0^t d\tau \cos[2\varphi_-(\tau)+eV\tau]}$. The two factors $\tilde{Z}_{mn}$ and $Z_{mn}$ correspond to the local density interaction and tunneling-induced backaction, respectively. The only nontrivial evolution of the reduced density matrix is in its off-diagonal terms with $m \neq n$, which take, up to a time-independent prefactor, the form

$$Z_{12} \propto e^{-[\Gamma(t)+i\Delta(t)]t}, \tag{9}$$

$$\tilde{Z}_{12} \propto e^{-[\tilde{\Gamma}(t)+i\tilde{\Delta}(t)]t}. \tag{10}$$

We identify the respective contributions to the induced energy shift, $\Delta(t)$ and $\tilde{\Delta}(t)$, and decoherence, $\Gamma(t)$ and $\tilde{\Gamma}(t)$. These are generically time-dependent quantities. In the following, we will focus separately on these contributions to the induced total decoherence $\Gamma_{\rm tot}(t) = \Gamma(t) + \tilde{\Gamma}(t)$, which characterize the properties of the QPC as a detector.

### A. Local density contribution

The term $Z_{12} = Z_{21}^*$ corresponds to a local change in the electrostatic potential caused by the DQD (see Appendix A), a fact known to lead to an "orthogonality catastrophe" in fermionic systems. The term "orthogonality catastrophe" refers to the vanishing, in the thermodynamic limit, of the overlap between the system's ground states before and after the change in the potential [36]. The average in $Z_{12}$ involves only the $\varphi_+$-dependent part of the free LL Hamiltonian. Since the latter is quadratic [cf. Eqs. (5) and (2)], we can directly write

$$Z_{12}(t) = e^{-\frac{1}{2}[\frac{g(\lambda_2-\lambda_1)}{\Lambda_g}]^2\langle[\varphi_+(t)-\varphi_+(0)]^2\rangle}. \tag{11}$$

The two-point correlation function of $\varphi_+$ is computed in Appendix B. In the long-time limit $t \gg 1/T$, $\Gamma(t)$ is independent of time, and we find that the local-density-induced decoherence rate is given by

$$\Gamma = \frac{g}{2}\pi T\left[\frac{(\lambda_2-\lambda_1)}{\Lambda_g}\right]^2. \tag{12}$$

This result is consistent with the known noninteracting ($g = 1$) orthogonality exponent in Luttinger systems [31,37]. Hence we see that for repulsive interactions, the factor $g < 1$ decreases this decoherence rate with respect to the noninteracting case. In a fermionic picture, the orthogonality catastrophe can be seen as a consequence of a "shake up" of the Fermi sea due to a change in the local potential. Intuitively, for strong repulsive interactions the electrons will redistribute after the potential change in order to minimize the interaction, consequently minimizing the effect of the shakeup. As expected, higher temperatures lead to a higher decoherence rate. The limit $T \to 0$ leads to the known power-law decay of the coherence factor, $Z_{mn}$, and hence to logarithmic corrections to the total decoherence rate, $\Gamma_{\rm tot}(t)$. It should be noted that this result corresponds to an equilibrium ($eV = 0$) contribution to the orthogonality catastrophe. This is due to the separable character of the reduced density matrix in the weak tunneling limit [cf. Eq. (6)]. In this limit, nonequilibrium effects are entirely contained in the tunneling term, as calculated in the next subsection.

### B. Tunneling term

The effect of the change in the transmission of the QPC due to the charge state of the DQD is encoded in $\tilde{Z}_{12} = \tilde{Z}_{21}^*$. We evaluate this quantity via a cumulant expansion. For simplicity of notation, we introduce the function

$$A_{\xi(\tau)}(\tau) = \cos\left[2\varphi_-(\tau) + eV\tau + \frac{\xi(\tau)}{2}\right], \tag{13}$$

where $\xi$ is a counting field whose role will be elucidated in the next section; for the remainder of this section, we set $\xi = 0$.

We evaluate the time-ordered products to obtain

$$\begin{aligned}\tilde{Z}_{12}(t) \approx 1 &+ \tilde{\lambda}_1\tilde{\lambda}_2\int_0^t d\tau\int_0^t d\tau'\langle A_0(\tau)A_0(\tau')\rangle \\ &- \tilde{\lambda}_1^2\int_0^t d\tau\int_0^\tau d\tau'\langle A_0(\tau)A_0(\tau')\rangle \\ &- \tilde{\lambda}_2^2\int_0^t d\tau\int_\tau^t d\tau'\langle A_0(\tau)A_0(\tau')\rangle.\end{aligned} \tag{14}$$

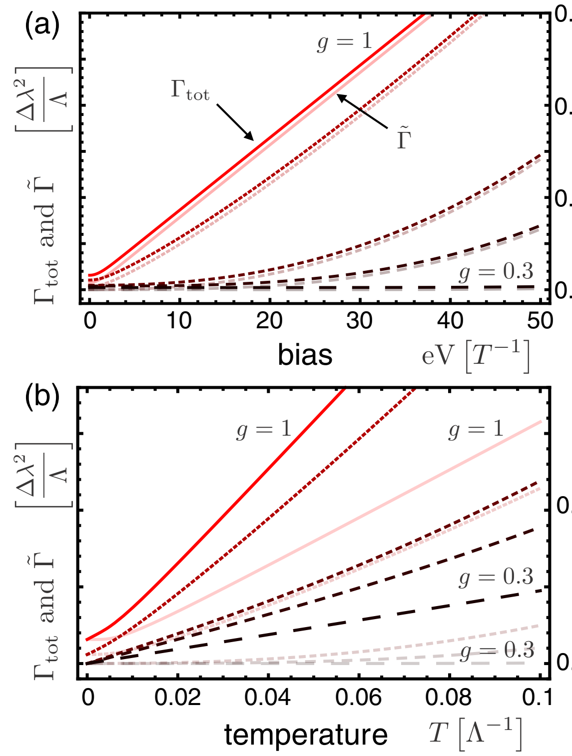


FIG. 2. Detection-induced decoherence: total decoherence $\Gamma_{\rm tot} = \tilde\Gamma + \Gamma$ (solid color) and tunneling-induced decoherence $\tilde\Gamma$ (shaded color) as a function of (a) voltage bias and (b) temperature—cf. Eqs. (15) and (12). All plots are for increasing interaction strength $g = 1, 0.9, 0.6, 0.5, 0.3$ from light to dark red and from continuous to coarsely dashed. The local-density-induced decoherence rate $\Gamma$ in our model is independent of bias and proportional to temperature; cf. Eq. (12). Hence it produces just a constant shift of the total rate $\Gamma_{\rm tot}$ in (a) while it modifies the slope in (b). We have set $\frac{T}{\Lambda_g} = 0.01$ in panel (a) and $\frac{eV}{\Lambda} = 0.01$ in panel (b). In all plots, $\tilde\lambda_2 - \tilde\lambda_1 = \lambda_2 - \lambda_1 = \Delta\lambda$.

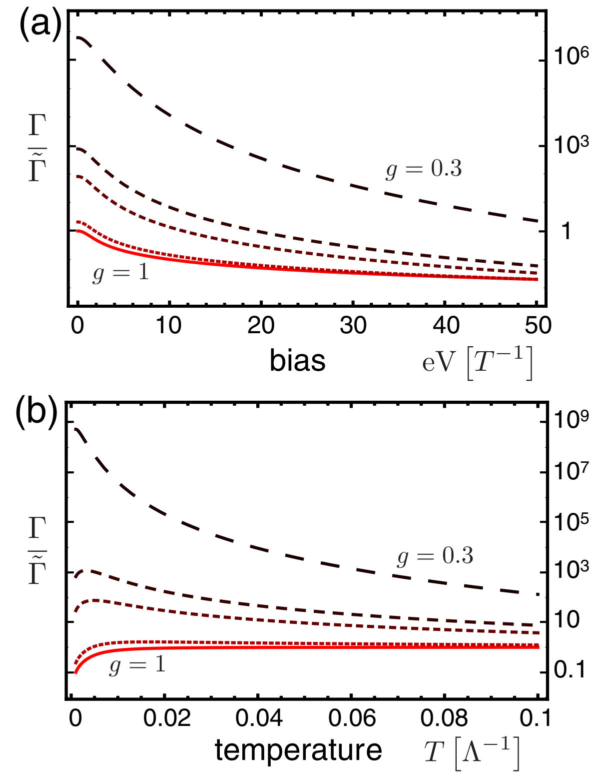


FIG. 3. Log-plot of the ratio between local-density-induced and tunneling-induced decoherence as a function of (a) bias voltage and (b) temperature; cf. Eqs. (12) and (15). For increasing interaction strength $g = 1, 0.9, 0.6, 0.5, 0.3$ from light to dark red and from continuous to coarsely dashed. $\frac{T}{\Lambda_g} = 0.01$ in (a) and $\frac{eV}{\Lambda_g} = 0.01$ in (b), $\tilde\lambda_2 - \tilde\lambda_1 = \lambda_2 - \lambda_1 = \Delta\lambda$.

As shown in Appendix C, we can express $\tilde Z_{12}(t)$ in terms of the well-known time-ordered correlator [38] $f^T(\tau - \tau') \equiv \langle \mathcal{T}_t\, e^{2i\varphi_-(\tau)} e^{-2i\varphi_-(\tau')}\rangle$. In the long-time limit $t \gg 1/T,\ 1/eV$, we obtain the contribution to the decoherence,

$$\tilde\Gamma(t) \approx \tfrac{1}{2}(\tilde\lambda_2 - \tilde\lambda_1)^2 \mathrm{Re}\{J_C\}, \tag{15}$$

where $J_C = \int_0^\infty ds\, f^T(s)\cos(eVs)$ [see Eq. (C5)]. $J_C$ is evaluated in Appendix D [Eq. (D6)], and it yields the explicit expression for the (time-independent) decoherence rate,

$$\tilde\Gamma = \frac{(\tilde\lambda_2 - \tilde\lambda_1)^2}{4\Lambda_g}\left(\frac{2\pi T}{\Lambda_g}\right)^{2/g-1} \times \frac{\left|\mathit{\Gamma}\left(\frac{1}{g} + i\frac{eV}{2\pi T}\right)\right|^2}{\mathit{\Gamma}\left(\frac{2}{g}\right)}\cosh(eV/2T), \tag{16}$$

where $\mathit{\Gamma}(x)$ is the Gamma function (note the cursive font, not to be confused with the local-density-induced decoherence rate $\Gamma$). The behavior of $\tilde\Gamma$ is plotted in Fig. 2 as a function of bias voltage and temperature for different values of the interaction strength $g$. As expected, $\tilde\Gamma$ increases both as a function of bias and temperature, reflecting the increase in shot and thermal noise, respectively. Upon increasing the interaction strength (corresponding to decreasing $g$), however, the decoherence generally *decreases*, i.e., electron-electron interactions reduce the measurement-induced backaction. Intuitively, this can be seen as a consequence of an increased "antibunching" of the electrons with increasing repulsive interactions, which leads to a suppression of tunneling events between the two sides of the QPC. Since the tunneling processes control the system detector coupling, their suppression results in a reduced backaction onto the DQD. For $g = 1$, Eq. (16) recovers the known result for the decoherence induced by noninteracting electrons in the tunneling regime. In particular, for $T \ll eV$, $\tilde\Gamma \approx \frac{eV}{4\pi v_F^2}(t_2 - t_1)^2$ [8,31,33], where $t_n$ are the tunneling strengths introduced in Eq. (4).

### C. Total decoherence

From the results presented in the previous two subsections, we see that the total decoherence $\Gamma_{\rm tot}$ is generically suppressed by increasing repulsive interactions. This is plotted in Fig. 2. Albeit both $\Gamma$ and $\tilde\Gamma$ are suppressed, this suppression is much stronger in the tunneling-induced decoherence $\tilde\Gamma$, leading to a variation of the ratio $\Gamma/\tilde\Gamma$ by several orders of magnitude depending on interactions, as shown in Fig. 3. For instance, for $eV \ll T \ll \Lambda_g$, we can analytically approximate

$$\frac{\Gamma}{\tilde{\Gamma}} \simeq \left(\frac{\lambda_1-\lambda_2}{\tilde{\lambda}_1-\tilde{\lambda}_2}\right)^2 \frac{2}{\sqrt{\pi}}\left(\pi\frac{T}{\Lambda_g}\right)^{2-\frac{2}{g}}\sqrt{g}, \tag{17}$$

showing a strong dependence of the ratio on the interactions ($T \ll \Lambda_g$). The strength of this effect is suppressed at larger voltage bias or temperature.

The reason behind this behavior is the decreasing strength of the tunneling term in Eq. (4) as compared to the local density interaction one in the effective low-energy behavior. The decoherence is generically dictated by the low-frequency correlations of the bath coupled to the system [39,40] (in our case, the Luttinger liquid detector), hence by the dynamics of the low-frequency modes of the bath. When tracing out the fast (high-energy) modes of the Luttinger liquid detector, the effective low-energy tunneling term is suppressed as compared to the local density term. This suppression is more prominent for stronger repulsively interacting systems, as shown by Kane and Fisher [35,41,42]. This leads to a divergent ratio $\Gamma/\tilde{\Gamma} \to \infty$ when $T \to 0$ and $eV \to 0$ simultaneously. When going to higher temperatures or higher voltages, the relative strength of the two contributions evolves toward comparable values (set by the bare constants $\tilde{\lambda}_n, \lambda_n$).

## IV. FULL COUNTING STATISTICS AND RATE OF ACQUISITION OF INFORMATION

The backaction of the detector on the measured system has to be compared with the ability of the detector to discriminate the different charge states of the DQD. For a given charge eigenstate ($n = 1,2$) of the double dot, the response of the detector is fully characterized by the probability distribution $\mathcal{P}_n(N,t)$ of a charge $q = eN$ to be transmitted through the tunnel junction in a fixed time interval $t$. The rate of acquisition of information on the charge state of the DQD is quantified by the statistical quantity [33]

$$\mathcal{M}(t) \equiv e^{-W(t)t} \equiv \sum_N \sqrt{\mathcal{P}_1(N,t)\mathcal{P}_2(N,t)}, \tag{18}$$

which measures how distinguishable the two distributions are.

The probability distribution $\mathcal{P}_n(N,t)$ is equivalently and conveniently characterized by the corresponding generating function $\chi_n(\xi,t) \equiv \sum_N \mathcal{P}_n(N,t)e^{i\xi N}$, the so called full counting statistics (FCS). The generating function can be expressed directly in terms of quantum averages of the tunneling operator [43],

$$\chi_n(\xi,t) = e^{W_n(\xi,t)t} = \left\langle \mathcal{T}_K \exp\left\{i\tilde{\lambda}_n \int_{\mathcal{C}_K} d\tau\, A_{\xi(\tau)}(\tau)\right\}\right\rangle, \tag{19}$$

where the time ordering $\mathcal{T}_K$ occurs on the Keldysh contour $\mathcal{C}_K$, and $\xi(\tau) = \pm\xi$ is the counting field introduced in Eq. (13). The FCS of interacting electrons is known in some cases, e.g., in quantum dots or diffusive conductors [44]. Here we consider instead Luttinger liquids. In the present situation of a tunneling Hamiltonian, the counting field enters as a phase of the tunneling operators [43] $t \to te^{i\xi(t)/2}$, $t^* \to t^*e^{-i\xi(t)/2}$. In this case, the counting field is a pure quantum field, i.e., $\xi(\tau) = \pm\xi$ is antisymmetric on the forward and backward branch of the Keldysh contour.

The generating function $\chi_n(\xi)$ in Eq. (19) is a generalization of $\tilde{Z}_{nn}(t)$ in Eq. (8), which includes the quantum field $\xi(\tau)$. As we did in the previous section for $\tilde{Z}_{12}(t)$, we evaluate $\chi_n(\xi)$ to second order in a cumulant expansion. In the long-time limit ($t \gg 1/T, 1/eV$), the Markovian nature of the electron transfer processes guarantees that the leading contribution to the cumulant-generating function is linear in time, i.e., $W_n(\xi,t) \approx W_n(\xi)$ is independent of $t$. We obtain

$$W_n(\xi) = \tilde{\lambda}_n^2[(\cos\xi - 1)\mathrm{Re}\{J_C\} - i\sin\xi\,\mathrm{Im}\{J_S\}], \tag{20}$$

where $J_S = \int_0^\infty ds\, f^T(s)\sin(eVs)$ is calculated in Appendix D. In this limit, the rate of acquisition of information $W(t)$ can be expressed directly in terms of $W_n(\xi)$ as [33]

$$W(t) = W \approx -\tfrac{1}{2}\min_{x\in\mathbb{R}}\{W_1(-ix) + W_2(+ix)\}, \tag{21}$$

where $W$ can be directly evaluated from Eq. (20) to be $W \approx \mathrm{Re}\{J_C\}\tilde{\lambda}_+ - \sqrt{(\mathrm{Re}\{J_C\}\tilde{\lambda}_+)^2 - (\mathrm{Im}\{J_S\}\tilde{\lambda}_-)^2}$, with $\tilde{\lambda}_- \equiv (\tilde{\lambda}_2^2 - \tilde{\lambda}_1^2)/2$, $\tilde{\lambda}_+ \equiv (\tilde{\lambda}_2^2 + \tilde{\lambda}_1^2)/2$, and $0 < \lambda_- < \lambda_+$. From the expression for $J_S$ in Appendix D, we obtain

$$W = \mathrm{Re}\{J_C\}[\lambda_+ - \sqrt{\lambda_+^2 - (\tanh[eV/2T]\,\lambda_-)^2}]. \tag{22}$$

In the next section, we discuss the implications of this result for the quantum measurement process. We note here that the acquisition of information is independent of the local density interaction contributions (parametrized by $\lambda_n$), since these do not affect the current and hence do not contribute to the gain of knowledge about the charge state of the DQD.

## V. EFFECTS ON QUANTUM-LIMITED DETECTION

The efficiency of the quantum measurement is characterized by the ratio

$$Q \equiv W/\Gamma_{\mathrm{tot}} = W/(\Gamma + \tilde{\Gamma}) \leqslant 1. \tag{23}$$

This definition takes into account only the decoherence on the measured system due to the measurement process, following the approach used for noninteracting detectors. $Q = 1$ corresponds to a quantum-limited detector. External, system-dependent decoherence mechanisms are outside the scope of this paper.

The efficiency $Q$ is properly defined for sufficiently long times $t > 1/T$, $1/eV$, where $Z_{mn}(t)$ and $\tilde{Z}_{mn}(t)$ are exponentially decaying in time and $W(t) = W$. With the help of Eqs. (15) and (22), we conveniently rewrite $Q$ as

$$Q = \frac{\frac{1+\eta^2}{2\eta^2}\left[1 - \sqrt{1 - \left(\frac{2\eta}{1+\eta^2}\tanh(eV/2T)\right)^2}\right]}{(1 + \Gamma/\tilde{\Gamma})}, \tag{24}$$

where $\eta = (\tilde{\lambda}_2 - \tilde{\lambda}_1)/(\tilde{\lambda}_1 + \tilde{\lambda}_2)$ characterizes how strong the electron tunneling is influenced by the different occupation of the DQD. It can be shown that $Q \leqslant 1$ and finite for $\eta \to 0$.

From Eqs. (22) and (15), we note that $W \propto \tilde{\Gamma} \propto \mathrm{Re}\{J_C\}$, where all interaction effects (characterized by $g$) are contained in the function $\mathrm{Re}\{J_C\}$. Therefore, in the absence of a local density contribution ($\lambda_1 = \lambda_2$, so $\Gamma = 0$), $Q$ is independent of $g$ and hence interactions have no effect on the quality of the detection process. The efficiency $Q$ for $\Gamma = 0$ is plotted in Figs. 4(a) and 4(b). In particular, for $T \ll eV$ (and $T \neq 0$)

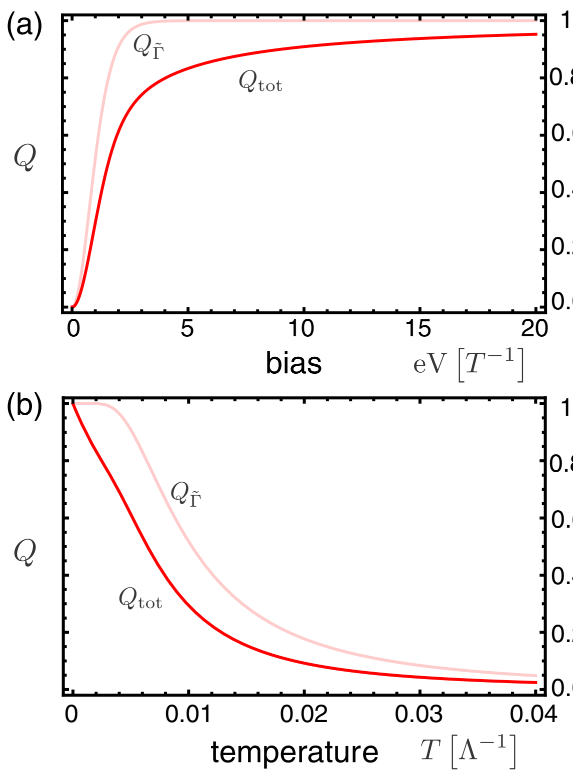


FIG. 4. Detector efficiency for the noninteracting case. Total efficiency, $Q_{\rm tot} = W/\Gamma_{\rm tot}$ (solid line), and efficiency without decoherence due to the local density interaction, $Q_{\tilde\Gamma} = W/\tilde\Gamma$ (shaded line), as a function of (a) bias voltage and (b) temperature. $Q_{\tilde\Gamma}$ is independent of $g$ and therefore valid also for the interacting case. With $\eta = 0.5$, $\tilde\lambda_2 - \tilde\lambda_1 = \lambda_2 - \lambda_1$, $\frac{T}{\Lambda_g} = 0.01$ in (a), and $\frac{eV}{\Lambda_g} = 0.01$ in (b).

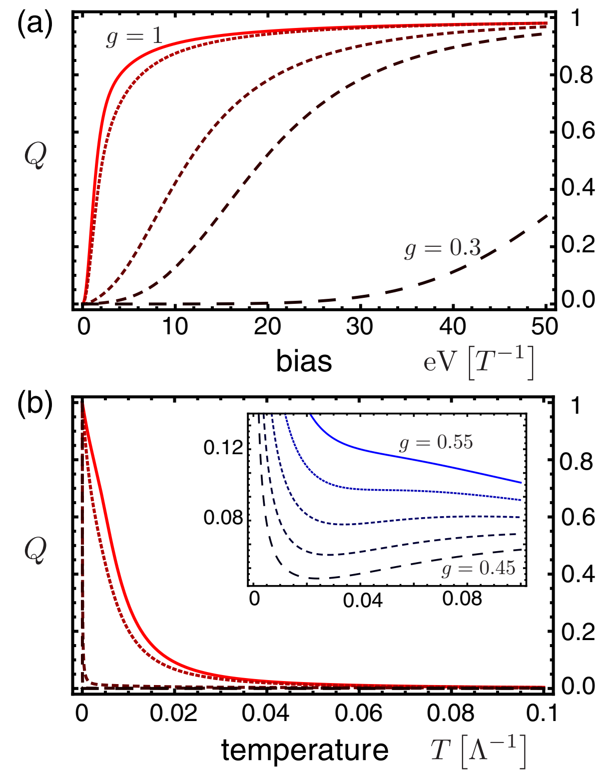


FIG. 5. Total detector efficiency $Q$ for the interacting case as a function of the applied bias (a) and temperature (b). Different curves from light to dark red and from continuous to coarsely dashed are for increasing interaction strengths, $g = 1, 0.9, 0.6, 0.5, 0.3$. The figures show a strong dependence of $Q$ on $g$ once orthogonality effects are considered. The inset in (b) shows a zoom-in of the crossover regime between monotonous and nonmonotonous temperature dependence for $g \sim 0.5$ ($g = 0.55, 0.525, 0.5, 0.475, 0.45$ from light to dark blue and from continuous to coarsely dashed). We used $\eta = 0.5$, $\tilde\lambda_2 - \tilde\lambda_1 = \lambda_2 - \lambda_1$, and $\frac{T}{\Lambda_g} = 0.01$ in (a), and $\frac{eV}{\Lambda_g} = 0.01$ in (b).

the detector is quantum-limited, $Q \to 1$, and it remains so in the presence of interactions. Repulsive interactions do have an effect in reducing the backaction (cf. Fig. 2), but the rate of acquisition of information is reduced by an equal amount. All in all, in the absence of a local density interaction, interactions leave the detector still quantum-limited, but they slow down the detection process. As for noninteracting QPC detectors, the efficiency of the detection is controlled only by $eV/T$, and in the limit of high temperature, thermal fluctuations induce unwanted backaction unaccompanied by information gain, driving the detector away from its quantum limit [cf. Figs. 4(a) and 4(b)].

Therefore, the local density interaction is essential to appreciate the effect of interactions. Once it is taken into account, lower temperatures are required to bring the detector to the quantum limit, even in the absence of interactions (see Fig. 4). This is due to the fact that this term provides no information gain, but it still induces decoherence in the system [31]. We showed in Sec. III B that decoherence due to the local density interactions *and* decoherence due to tunneling are diminished by interactions, but in a very unequal way. The suppression of the tunneling-induced decoherence $\tilde\Gamma$ due to electron-electron interactions is much more pronounced than that of the decoherence caused by the local density contribution, $\Gamma$. Since $W \propto \tilde\Gamma$, the acquisition of information is suppressed in the same manner. This leads to a strong suppression of the measurement efficiency $Q$ [Eq. (24)] for repulsive interactions with respect to the noninteracting case. Interaction effects do not eliminate the monotonously increasing dependence on the voltage bias of $Q$ [cf. Fig. 5(a)], but they can delay the saturation to the quantum limit $Q = 1$ to very high voltages or very low temperatures for strongly repulsively interacting systems.

Surprisingly the temperature dependence of $Q$ shows an interesting nonmonotonous feature depending on interactions. For a noninteracting system, $Q$ is a monotonously decreasing function of temperature, reflecting the fact that increasing thermal fluctuations induce extra decoherence without a corresponding gain of information about the system's state [cf. Fig. 4(b)]. However, we find that for strong interactions and at high temperatures with respect to the bias, $Q$ increases with $T$ in an intermediate regime. Specifically, for $0 < eV \ll T < \frac{\Lambda_g}{2\pi}\left(\frac{\Gamma(\frac{1}{g})^2(\tilde\lambda_1-\tilde\lambda_2)^2}{g\Gamma(\frac{2}{g})(\lambda_1-\lambda_2)^2}\right)^{\frac{g}{2g-2}} \ll \Lambda_g$, we have

$$Q \simeq \frac{(\tilde\lambda_1 - \tilde\lambda_2)^2\, \Gamma\left(\frac{1}{g}\right)^2}{(\lambda_1 - \lambda_2)^2(\eta^2+1)g\,\Gamma\left(\frac{2}{g}\right)}\left(\frac{2\pi}{\Lambda_g}\right)^{2/g-2}(eV)^2 T^{\frac{2}{g}-4}. \tag{25}$$

The expression shows a crossover between an increasing and a decreasing function of $T$ for $g \simeq 1/2$ [cf. also the inset in Fig. 5(b)]. This feature emerges from the competition between two effects of increasing temperature: (i) an increase of thermal fluctuations and (ii) a increasing prominence of the tunneling term compared to the local density one [cf. Fig. 3(b)]. To highlight these competing effects, we can write the efficiency in Eq. (24) as $Q = Q_0/(1 + \Gamma/\tilde{\Gamma})$, so that $Q_0$ is a monotonously decreasing function of temperature. At low energies, decoherence is dominated by the local density term due to suppression of tunneling, and we can roughly write $Q \sim Q_0(\tilde{\Gamma}/\Gamma)$. While the thermal fluctuations reduce $Q$, the growing prominence of the tunneling term increases the weight of the "information carrying" part of the interaction Hamiltonian, hence increasing $Q$. When (ii) is dominant compared to (i), $Q$ increases with temperature. This is controlled by the parameters of the detector. In particular, since the temperature dependence of the relative strength between local density and tunneling contributions in the detector is strong for strong interaction, the increasing behavior of $Q$ with $T$ is possible only for sufficiently small $g$. The inset in Fig. 5(b) shows a zoom into the critical regime of the crossover between monotonous and nonmonotonous temperature dependence.

## VI. CONCLUSIONS AND OUTLOOK

In this paper, we analyzed the effects of interactions on the efficiency of quantum detection. We executed our analysis for two voltage-biased electron reservoirs connected by a tunnel junction, whose current serves as a charge detector of a proximate charge qubit. We included electron-electron interactions by modeling the leads as Luttinger liquids, and we incorporated the effects of local density fluctuations due to the charge qubit, besides its effect on the tunneling amplitude. The model is of interest both for charge-sensing schemes used in experiments and as a theoretical paradigm case study.

We found that interactions reduce the induced decoherence on the measured system, along with the rate of acquisition of information. In the absence of a local density interaction term, both acquisition of information and tunneling-induced decoherence are suppressed in the same manner by interactions. In this case, interactions do not alter the efficiency of the detector, which tends to be quantum-limited at low temperature, but they slow down its response. Once the local-density-induced decoherence is considered, interactions do play a role for the efficiency, reducing it with respect to the noninteracting case.

The relative contributions of tunneling and local-density-induced decoherence are strongly affected by interactions, and the local density contribution can dominate at low temperature and voltage bias for strong interactions. This is a consequence of the downward renormalization of the tunneling term for repulsive interactions at low energies. The same renormalization is responsible for the slower rate of acquisition of information in the interacting case. This renormalization is less pronounced for increasing energy, resulting in a tendency to an increased acquisition of information rate. As a result of the interplay between these effects, we have identified an intermediate temperature regime where, for sufficiently strong interactions ($g \lesssim 1/2$), the detector efficiency *increases* with temperature. This has to be contrasted with the weakly interacting case in which increasing thermal fluctuations monotonously reduce the detector's efficiency. As a function of the voltage bias, repulsive interactions delay the quantum limit $Q = 1$ to increasingly higher voltages (or lower temperatures). This is purely a consequence of the local density interaction.

Our models captures the effects of interactions in the simplest experimentally relevant configuration. As such, it has limitations and poses interesting future challenges, which we outline briefly here. Our results allow us to assess the efficiency of the detector due to processes inherent to the measurement itself, which are unavoidable as long as the system is coupled to the detector for readout. The readout efficiency will also be affected by other external decoherence mechanisms extraneous to the measurement process. These have to be dealt with separately and are system-specific. For instance, one can come up with more efficient qubit designs or environment engineering to minimize the coupling to specific decoherence sources. Moreover, in our model we assumed full control of the tunneling matrix element between the dots, which allowed us to set $\gamma$ smaller than all the other energies in the model after preparing the initial coherent state. Our results are valid for $t \ll 1/\gamma$ such that we can effectively consider $\gamma = 0$. Experimentally, the required degree of control is available for charge qubits, though with more sophisticated designs than a double quantum dot [21–23], and for spin qubits whose spin state is read by quantum point contacts via spin-to-charge conversion mechanisms [25,26]. The protocol we analyze has to be considered as a test for the detector's properties. In fact, based on the results for noninteracting systems [8], there are reasons to expect that the parameters for which the detector is found to be quantum-limited in our paper make the detector quantum-limited also in the presence of interdot tunneling. The argument is that the efficiency is a property of the measurement process and the detector, not of the qubit's dynamics. A proper analysis of the dot-detector coupling in the presence of finite interdot tunneling is a key future point to address, especially because this is the regime where measurement-based control of the qubit dynamics can operate. One can anticipate, for instance, that pure decoherence will be accompanied by relaxation processes. We have also modeled the DQD as single-level dots with a single occupation, which is the simplest experimentally relevant case. Considering double occupation requires a treatment with a larger qubit Hilbert space, and therefore addressing the coherences of different off-diagonal terms, which is outside of the scope of this paper but would be an interesting follow-up problem. Lastly, the nonmonotonic behavior of the efficiency $Q$ with temperature is present for strong interactions, $g \lesssim 1/2$. Although this is an experimentally challenging regime, recent experiments in different platforms have shown evidence of Luttinger liquid behavior with interactions up to $g \approx 0.2$ [46–48].

## ACKNOWLEDGMENTS

The work is supported by Deutsche Forschungsgemeinschaft under Grant No. RO4710/1-1 and the SFB 658 (A.B.). S.V.K. acknowledges support from ERC-StG OPTOMECH.

## APPENDIX A: COUPLING HAMILTONIAN

We model the electrostatic coupling of the DQD to the interacting QPC to include two effects: a coupling of the electron on the DQD to the local electronic density at the end ($x = 0$) of the two Luttinger liquid leads that depends on the charge state of the DQD, and a state-dependent tunneling between the two sides of the QPC. To derive the interaction Hamiltonian Eq. (4), we start from the fermionic representation

$$H_{\rm int} = \sum_{n,j,c} \alpha_n : \Psi^\dagger_{c,j}\Psi_{c,j}(0,t) : c^\dagger_n c_n + [t_n : \Psi^\dagger_{2,L}\Psi_{1,R}(0,t) : + t_n^* : \Psi^\dagger_{2,R}\Psi_{1,L}(0,t) :] c^\dagger_n c_n, \tag{A1}$$

where $\Psi^\dagger_{c,j}(x,t)$ [$\Psi_{c,j}(x,t)$ ] creates (annihilates) an electron at position $x$ and time $t$, with chirality $c = 1,2$ and on side $j = L,R$ [note that $c = 1$ ($c = 2$) indicates moving toward (away from) the QPC]. $n = 1,2$ indicates the state of the DQD, and $: \cdots :$ denotes normal ordering. These fermionic fields can be written in terms of the bosonic operators as

$$\Psi_{c,j} = \frac{\eta_{c,j}}{\sqrt{2\pi a_0}} e^{ick_F x} e^{\mp ieVt/2} e^{i(c\theta_j + \varphi_j)}, \tag{A2}$$

where all fields are evaluated at $(x,t)$. $\eta_{c,j}$ are Klein factors, $k_F$ is the Fermi momentum, the $\mp$ in the exponential corresponds to $R$ $(-)$ and $L$ $(+)$, and $eV = \mu_L - \mu_R$.

We consider the tunneling term as a perturbation on the two $(L,R)$ disconnected LL systems. Without tunneling, the QPC acts as a strong impurity that imposes that the density fluctuations vanish at $x = 0$. This boundary condition results in [38,42]

$$\theta_L(x = 0,t) = \theta_R(x = 0,t) = 0\,. \tag{A3}$$

Using this condition together with $t_n = t_n^*$ and substituting Eq. (A2) into Eq. (A1), we obtain straightforwardly the second term in Eq. (4), with $\tilde{\lambda}_n = t_n/(\pi a_0)$.

It is furthermore convenient to write the bosonic fields in the interaction representation, in which the bosonic fields evolve according to the free Hamiltonian $H_{\rm LL}$, Eq. (2), and switch to the description in terms of sum and difference fields, $\theta_\pm = 1/2[\theta_L \pm \theta_R]$ and $\varphi_\pm = 1/2[\varphi_L \pm \varphi_R]$. Using the commutators ($\alpha = \pm$)

$$[\theta_\alpha(x),\varphi_{\alpha'}(x')] = \frac{i\pi}{4}\,{\rm sgn}(x - x')\delta_{\alpha,\alpha'},$$
$$[\theta_\alpha(x),\partial_{x'}\varphi_{\alpha'}(x')] = -\frac{i\pi}{2}\delta(x - x')\delta_{\alpha,\alpha'}, \tag{A4}$$

we obtain the free Heisenberg equation of motion

$$\dot{\varphi}_\pm(x,t) = -\frac{v_g}{g}\partial_x\theta_\pm(x,t), \tag{A5}$$

$$\dot{\theta}_\pm(x,t) = -g v_g \partial_x\varphi_\pm(x,t). \tag{A6}$$

The first term in Eq. (A1), which is the density-density electrostatic interaction between the dot and the LL at $x = 0$, can easily be bosonized using the identity $\rho_j = \sum_c : \Psi^\dagger_{c,j}\Psi_{c,j} := \partial_x\theta_j/\pi$ for the normal ordered density (i.e., the density of charge fluctuations). Using Eq. (A5), we can express $\partial_x\theta_j$ in terms of $\dot{\varphi}_j$ and we obtain the first interaction term in Eq. (4) with $\lambda_n = \frac{2\alpha_n}{\pi a_0}$.

Finally, Eq. (A5) allows us to write $\tilde{H}^n_{\rm int} = \langle n|\tilde{H}_{\rm int}|n\rangle$ in terms of phase fields only,

$$\tilde{H}^n_{\rm int}(t) = -g\frac{\lambda_n}{\Lambda_g}\dot{\varphi}_+(t) + \tilde{\lambda}_n \cos[2\varphi_-(t) + eVt], \tag{A7}$$

with $\Lambda_g = v_g/a_0$ the high-energy cutoff.

## APPENDIX B: CALCULATION OF $Z(t)$

The detector's contribution to the evolution of the off-diagonal terms of the density matrix is expressed in terms of averages of the detector's fields in Eqs. (11) and (14). We compute here these averages, $\langle[\varphi_\pm(t) - \varphi_\pm(0)]^2\rangle$. An alternative calculation of the same average can be found in Ref. [38]. To proceed, it is useful to write the phase fields in terms of bosonic operators in the interacting basis,

$$\varphi_\pm(x,t) = i\sqrt{\frac{\pi}{2Lg}}\sum_{k\neq 0}\frac{e^{-|k|a_0/2}}{\sqrt{|k|}}[e^{-ipx}b^\dagger_{k,\pm}(t) - e^{ipx}b_{k,\pm}(t)], \tag{B1}$$

where we have introduced the standard high-energy cutoff $\exp(-|k|a_0/2)$. The bosonic creation (destruction) operators $b^\dagger_k(t)$ [$b_k(t)$] are of the form

$$b^\dagger_{k,\pm}(t) = b^\dagger_{k,\pm}(0)e^{iv_g t|k|},$$
$$b_{k,\pm}(t) = b_{k,\pm}(0)e^{-iv_g t|k|}, \tag{B2}$$

where $b^\dagger_{k,\pm}(0)$ and $b_{k,\pm}(0)$ fulfill standard bosonic commutation relations ($\alpha,\alpha' = \pm$)

$$[b_{k,\alpha}(0),b^\dagger_{k',\alpha'}(0)] = \delta_{k,k'}\delta_{\alpha,\alpha'}. \tag{B3}$$

The free Hamiltonian of the Luttinger liquid in this representation is simply

$$H_{\rm LL} = \sum_{\alpha=\pm;k=0}^{\infty} v_g|k|b^+_{k,\alpha}(0)b_{k,\alpha}(0) \tag{B4}$$

and the vacuum expectation value

$$\langle b^+_{k,\alpha}(0)b_{k',\alpha'}(0)\rangle = n_b(k)\delta_{k,k'}\delta_{\alpha,\alpha'}, \tag{B5}$$

where $n_b(k) = [\exp(v_g|k|/T) - 1]^{-1}$ is the usual Bose-Einstein distribution at temperature $T$, with $k_B = 1$.

Using Eqs. (B1)–(B5), we can perform the vacuum expectation value by going to the continuum limit

$$\langle[\varphi_\pm(\tau) - \varphi_\pm(\tau')]^2\rangle = \frac{1}{g}I(\tau - \tau')$$
$$I(s) = \mathcal{P}\int_0^\infty \frac{dk}{k}e^{-a_0 k}[2n_b(k) + 1] \times [1 - \cos(v_g k s)], \tag{B6}$$

where $\mathcal{P}$ denotes the principal value of the integral.

We can divide the integral into a zero-temperature quantum term and a thermal term proportional to $n_B(v_g k)$. The quantum term can be calculated to be

$$\mathcal{P}\int_0^\infty \frac{dk}{k} e^{-a_0 k}[1-\cos(v_g k\tau)] = \frac{1}{2}\log\left[1+\left(\frac{v_g\,\tau}{a_0}\right)^2\right]. \tag{B7}$$

For the thermal contribution in turn we obtain

$$\mathcal{P}\int_0^\infty \frac{dk}{k} e^{-a_0 k}[1-\cos(v_g k\,\tau)]n_B(v_g k) \tag{B8}$$

$$= \frac{1}{2}\log\left(\frac{\Gamma\left(1+\frac{a_0}{\beta v_g}\right)^2}{\Gamma\left(1-i\frac{\tau}{\beta}+\frac{a_0}{\beta v_g}\right)\Gamma\left(1+i\frac{\tau}{\beta}+\frac{a_0}{\beta v_g}\right)}\right), \tag{B9}$$

where $\Gamma$ is the Gamma function. In the limit $\frac{a_0}{\beta v_g} \ll 1$ ($\beta = 1/T$), we obtain

$$\mathcal{P}\int_0^\infty \frac{dk}{k}[1-\cos(v_g k\tau)]n_B(v_g k) = \frac{1}{2}\log\left(\frac{\sinh\left(\frac{\pi\tau}{\beta}\right)}{\frac{\pi\tau}{\beta}}\right). \tag{B10}$$

To obtain Eq. (B10) we used $\Gamma(1-z)\Gamma(1+z) = z\Gamma(z)\Gamma(1-z) = z\pi/\sin(\pi z)$. Putting together the two contributions, we obtain

$$I(\tau) = \frac{1}{2}\log\left[1+\left(\frac{v_g\,\tau}{a_0}\right)^2\right] + \log\left(\frac{\sinh\left(\frac{\pi\tau}{\beta}\right)}{\frac{\pi\tau}{\beta}}\right) \tag{B11}$$

$$\simeq -\log\left[\frac{\frac{\pi a_0}{\beta v_g}}{\sinh\left(\frac{\pi\tau}{\beta}\right)}\right], \tag{B12}$$

where we approximated $\tau \gg \frac{a_0}{v_g} = \Lambda_g^{-1}$. Going to large times $\tau \gg \beta$,

$$I(\tau) \approx \log\left[\frac{\beta\Lambda_g}{2\pi}\right] + \frac{\pi\tau}{\beta}. \tag{B13}$$

Inserting the average into $Z_{mn}(t) = e^{-\frac{1}{2}\left[\frac{g(\lambda_n-\lambda_m)}{\Lambda_g}\right]^2\langle[\varphi_+(t)-\varphi_+(0)]^2\rangle}$ leads to

$$Z_{mn}(t) \approx \left(\frac{\beta\Lambda_g}{2\pi}\right)^{-\frac{g}{2}\left[\frac{(\lambda_n-\lambda_m)}{\Lambda_g}\right]^2} e^{-\Gamma t}, \tag{B14}$$

with the decoherence rate $\Gamma$ as given in Eq. (12).

## APPENDIX C: CALCULATION OF $\tilde{Z}_{12}(t)$ AND $\chi_n(\xi,t)$

We evaluate here the expressions in Eqs. (14) and (19). We make use of the fact that in expressions of the form $\langle e^{\pm 2i\phi_\pm(\tau)}e^{\pm 2i\phi_\pm}\rangle$, only "neutral" configurations of the kind

$$f(\tau-\tau') = \langle e^{2i\varphi_-(\tau)}e^{-2i\varphi_-(\tau')}\rangle = \langle e^{-2i\varphi_-(\tau)}e^{2i\varphi_-(\tau')}\rangle \tag{C1}$$

do not vanish [38]. Therefore, from Eq. (14),

$$\begin{aligned}\tilde{Z}_{12}(t) \approx 1 &+ \frac{\tilde{\lambda}_1\tilde{\lambda}_2}{2}\int_0^t d\tau\int_0^t d\tau' f(\tau-\tau')\cos\left[eV(\tau-\tau')\right]\\ &- \frac{\tilde{\lambda}_1^2}{2}\int_0^t d\tau\int_0^\tau d\tau' f(\tau-\tau')\cos\left[eV(\tau-\tau')\right]\\ &- \frac{\tilde{\lambda}_2^2}{2}\int_0^t d\tau\int_\tau^t d\tau' f(\tau-\tau')\cos\left[eV(\tau-\tau')\right].\end{aligned} \tag{C2}$$

Introducing new variables $s = \tau - \tau'$ and $r = (\tau+\tau')/2$, we can perform the integral over $r$ to obtain

$$\begin{aligned}\tilde{Z}_{12}(t) \approx 1 &+ \frac{\tilde{\lambda}_1}{2}(\tilde{\lambda}_2-\tilde{\lambda}_1)\int_0^t ds\,(t-s)f(s)\cos(eVs)\\ &+ \frac{\tilde{\lambda}_2}{2}(\tilde{\lambda}_1-\tilde{\lambda}_2)\int_{-t}^0 ds\,(t-s)f(s)\cos(eVs).\end{aligned} \tag{C3}$$

We note that

$$\begin{aligned}f(-s) &= \langle e^{2i\varphi(-s)}e^{-2i\varphi(0)}\rangle = \langle e^{2i\varphi(0)}e^{-2i\varphi(s)}\rangle\\ &= \langle e^{2i\varphi(s)}e^{-2i\varphi(0)}\rangle^* = f(s)^*,\end{aligned} \tag{C4}$$

where in the first equality we make use of the fact that the two-time correlation function depends only on the time difference. In the long-time limit ($t \gg 1/eV$), we retain only the dominant contribution for $t \to \infty$, i.e., the terms with the integrand $\propto t$ in Eq. (C3). Using $f(-s) = f(s)^*$, we can rewrite the integral in the positive domain $s > 0$ and then replace $f(s)$ by the time-ordered correlator $f^T(s) \equiv \langle \mathcal{T}e^{2i\varphi(s)}e^{-2i\varphi(0)}\rangle$, which is well-known in the literature [38]. We obtain

$$\begin{aligned}\tilde{Z}_{12}(t) \approx 1 &- \frac{(\tilde{\lambda}_2-\tilde{\lambda}_1)^2}{2}\,t\int_0^\infty ds\,\mathrm{Re}\{f^T(s)\}\cos(eVs)\\ &+ i\,\frac{(\tilde{\lambda}_2^2-\tilde{\lambda}_1^2)}{2}\,t\int_0^\infty ds\,\mathrm{Im}\{f^T(s)\}\cos(eVs).\end{aligned} \tag{C5}$$

Reexponentiating this expression in the form of Eq. (10) and disregarding the induced level shift $\tilde{\Delta}$, which leaves the measurement properties of the device unaffected, leads to Eq. (15) in the main text.

The calculation for the FCS function $W_n(\xi,t)$ proceeds in the same manner, replacing $A_0 \to A_\xi$ in Eq. (14) with $A_\xi$ defined in Eq. (13) and taking $\lambda_1 = \lambda_2 = \lambda_n$. We obtain

$$\begin{aligned}W_n(\xi,t)\,t = \frac{\tilde{\lambda}_n^2}{2}\int_0^t d\tau\int_0^t d\tau' f(\tau-\tau')\\ \times\mathrm{Re}[(e^{-i\xi}-1)e^{ieV(\tau-\tau')}],\end{aligned} \tag{C6}$$

which in the long-time limit $t \gg 1/eV$ leads to Eq. (20) in the main text.

## APPENDIX D: CALCULATION OF Re$\{J_C\}$ AND Im$\{J_S\}$

In this appendix, we calculate the time integrals $J_C$ and $J_S$ in Eqs. (15) and (20). We use the well-known form for the time-ordered correlation function [38] for positive times,

$$f^T(s>0) = \frac{\left(i\frac{\pi a_0}{\beta v_g}\right)^{2/g}}{\left(-\sinh\left[\frac{\pi}{\beta}(s-i0_+)\right]\right)^{2/g}} \tag{D1}$$

$$= \frac{\left(\frac{\pi a_0}{\beta v_g}\right)^{2/g}}{\left|\sinh^2\left[\frac{\pi}{\beta}t\right]\right|^{1/g}}e^{-i(\pi-0_+)/g}. \tag{D2}$$

Alternatively, this result can be obtained from noting that $f(\tau-\tau') = e^{-\frac{2}{g}I(\tau-\tau')}e^{2[\varphi_-(\tau),\varphi_-(\tau')]}$, where $I(s)$ was calculated in Appendix B. With this we can evaluate the real part of

$J_C$, needed for the decoherence Eq. (15). Explicitly,

$$\begin{aligned}\mathrm{Re}\{J_C\} &= \int_0^\infty ds\, \mathrm{Re}\{f^T(s)\}\cos(eVs)\\ &= \frac{1}{2}\cos\left(\frac{\pi}{g}\right)\left(\frac{\pi a_0}{\beta v_g}\right)^{2/g}\int_0^\infty ds\,\frac{1}{\sinh[\frac{\pi}{\beta}s]^{2/g}}(e^{ieVs}+e^{-ieVs})\\ &= \frac{1}{2}\cos\left(\frac{\pi}{g}\right)\left(\frac{2\pi a_0}{\beta v_g}\right)^{2/g}\frac{\beta}{2\pi}\left(\frac{\Gamma\left(\frac{1}{g}-i\frac{\beta}{2\pi}eV\right)\Gamma\left(1-\frac{2}{g}\right)}{\Gamma\left(1-\frac{1}{g}-i\frac{\beta}{2\pi}eV\right)}+\frac{\Gamma\left(\frac{1}{g}+i\frac{\beta}{2\pi}eV\right)\Gamma\left(1-\frac{2}{g}\right)}{\Gamma\left(1-\frac{1}{g}+i\frac{\beta}{2\pi}eV\right)}\right)\\ &= \frac{1}{2}\cos\left(\frac{\pi}{g}\right)\left(\frac{2\pi a_0}{\beta v_g}\right)^{2/g}\frac{\beta}{2\pi}\Gamma\left(1-\frac{2}{g}\right)2\,\mathrm{Re}\left(\frac{\Gamma(\frac{1}{g}+i\frac{\beta}{2\pi}eV)}{\Gamma\left(1-\frac{1}{g}+i\frac{\beta}{2\pi}eV\right)}\right),\end{aligned} \tag{D3}$$

where we dropped the positive infinitesimal $0_+$ and used

$$\int_0^\infty ds\,\frac{1}{\sinh\left[\frac{\pi}{\beta}t\right]^{2/g}}e^{i\omega t} = 2^{2/g}\frac{\beta}{2\pi}B\left(-i\frac{\beta}{2\pi}\omega+\frac{1}{g},1-\frac{2}{g}\right) \tag{D4}$$

with $B(x,y)=\frac{\Gamma(x)\Gamma(y)}{\Gamma(x+y)}$. Using the general identity of the $\Gamma$ function, $\Gamma(x)\Gamma(1-x)=\frac{\pi}{\sin(\pi x)}$, and some trigonometric identities, we can write this as

$$2\cos\left(\frac{\pi}{g}\right)\Gamma\left(1-\frac{2}{g}\right)\mathrm{Re}\left(\frac{\Gamma\left(\frac{1}{g}+i\frac{eV}{2\pi T}\right)}{\Gamma\left(1-\frac{1}{g}+i\frac{eV}{2\pi T}\right)}\right) = \frac{\left|\Gamma\left(\frac{1}{g}+i\frac{eV}{2\pi T}\right)\right|^2}{\Gamma\left(\frac{2}{g}\right)}\cosh(eV/2T), \tag{D5}$$

which leads to

$$\mathrm{Re}\{J_C\} = \frac{1}{2}\left(\frac{2\pi a_0}{\beta v_g}\right)^{2/g}\frac{\beta}{2\pi}\frac{\left|\Gamma\left(\frac{1}{g}+i\frac{eV}{2\pi T}\right)\right|^2}{\Gamma\left(\frac{2}{g}\right)}\cosh(eV/2T), \tag{D6}$$

in accordance with the results in Ref. [45]. From here the form of the decoherence rate $\tilde{\Gamma}$, Eq. (16), directly follows.

Similarly, $\mathrm{Im}\{J_S\}$ can be calculated to be

$$\begin{aligned}\mathrm{Im}\{J_S\} &= \int_0^\infty ds\,\mathrm{Im}\{f^T(s)\sin(eVs)\}\\ &= -\left(\frac{\pi a_0}{\beta v_g}\right)^{2/g}\sin\left(\frac{\pi}{g}\right)\int_0^\infty ds\,\frac{1}{\left|\sinh^2\left[\frac{\pi}{\beta}t\right]\right|^{1/g}}\frac{1}{2i}(e^{ieVs}-e^{-ieVs})\\ &= -\frac{1}{2i}\sin\left(\frac{\pi}{g}\right)\left(\frac{2\pi a_0}{\beta v_g}\right)^{2/g}\frac{\beta}{2\pi}\left(\frac{\Gamma\left(\frac{1}{g}-i\frac{\beta}{2\pi}eV\right)\Gamma\left(1-\frac{2}{g}\right)}{\Gamma\left(1-\frac{1}{g}-i\frac{\beta}{2\pi}eV\right)}-\frac{\Gamma\left(\frac{1}{g}+i\frac{\beta}{2\pi}eV\right)\Gamma\left(1-\frac{2}{g}\right)}{\Gamma\left(1-\frac{1}{g}+i\frac{\beta}{2\pi}eV\right)}\right)\\ &= \sin\left(\frac{\pi}{g}\right)\left(\frac{2\pi a_0}{\beta v_g}\right)^{2/g}\frac{\beta}{2\pi}\Gamma\left(1-\frac{2}{g}\right)\mathrm{Im}\left(\frac{\Gamma\left(\frac{1}{g}+i\frac{\beta}{2\pi}eV\right)}{\Gamma\left(1-\frac{1}{g}+i\frac{\beta}{2\pi}eV\right)}\right).\end{aligned}$$

Using again $\Gamma(x)\Gamma(1-x)=\frac{\pi}{\sin(\pi x)}$ and some trigonometric identities, we can write this as

$$-2\sin\left(\frac{\pi}{g}\right)\Gamma\left(1-\frac{2}{g}\right)\mathrm{Im}\left(\frac{\Gamma\left(\frac{1}{g}+i\frac{eV}{2\pi T}\right)}{\Gamma\left(1-\frac{1}{g}+i\frac{eV}{2\pi T}\right)}\right) = \frac{\left|\Gamma\left(\frac{1}{g}+i\frac{eV}{2\pi T}\right)\right|^2}{\Gamma\left(\frac{2}{g}\right)}\sinh(eV/2T), \tag{D7}$$

which sets the form of $\mathrm{Im}\{J_S\}$,

$$\mathrm{Im}\{J_S\} = \frac{1}{2}\left(\frac{2\pi a_0}{\beta v_g}\right)^{2/g}\frac{\beta}{2\pi}\frac{\left|\Gamma\left(\frac{1}{g}+i\frac{eV}{2\pi T}\right)\right|^2}{\Gamma\left(\frac{2}{g}\right)}\sinh(eV/2T). \tag{D8}$$

[1] A. A. Clerk, M. H. Devoret, S. M. Girvin, F. Marquardt, and R. J. Schoelkopf, Rev. Mod. Phys. **82**, 1155 (2010).

[2] H. Wiseman and G. J. Milburn, *Quantum Measurement and Control* (Cambridge University Press, Cambridge, 2010).

[3] A. Morello, J. J. Pla, F. A. Zwanenburg, K. W. Chan, K. Y. Tan, H. Huebl, M. Möttönen, C. D. Nugroho, C. Yang, J. A. van Donkelaar *et al.*, Nature (London) **467**, 687 (2010).
[4] S. Kagami, Y. Shikano, and K. Asahi, J. Phys. E **43**, 761 (2011).
[5] J. P. Groen, D. Ristè, L. Tornberg, J. Cramer, P. C. de Groot, T. Picot, G. Johansson, and L. DiCarlo, Phys. Rev. Lett. **111**, 090506 (2013).
[6] D. R. Ward, D. Kim, D. E. Savage, M. G. Lagally, R. H. Foote, M. Friesen, S. N. Coppersmith, and M. A. Eriksson, npj Quant. Inf. **2**, 16032 (2016).
[7] A. N. Korotkov, Phys. Rev. B **60**, 5737 (1999).
[8] A. N. Korotkov, Phys. Rev. B **63**, 115403 (2001).
[9] L. M. K. Vandersypen and I. L. Chuang, Rev. Mod. Phys. **76**, 1037 (2005).
[10] M. Shapiro and P. Brumer, *Quantum Control of Molecular Processes* (Wiley, Weinheim, 2012).
[11] O. Hosten and P. Kwiat, Science **319**, 787 (2008).
[12] P. B. Dixon, D. J. Starling, A. N. Jordan, and J. C. Howell, Phys. Rev. Lett. **102**, 173601 (2009).
[13] J. Dressel, M. Malik, F. M. Miatto, A. N. Jordan, and R. W. Boyd, Rev. Mod. Phys. **86**, 307 (2014).
[14] Q. Zhang, R. Ruskov, and A. N. Korotkov, Phys. Rev. B **72**, 245322 (2005).
[15] O. Zilberberg, A. Romito, D. J. Starling, G. A. Howland, C. J. Broadbent, J. C. Howell, and Y. Gefen, Phys. Rev. Lett. **110**, 170405 (2013).
[16] A. N. Jordan, J. Tollaksen, J. E. Troupe, J. Dressel, and Y. Aharonov, Quant. Stud.: Math. Found. **2**, 5 (2015).
[17] C. Meyer zu Rheda, G. Haack, and A. Romito, Phys. Rev. B **90**, 155438 (2014).
[18] R. Vijay, C. Macklin, D. H. Slichter, S. J. Weber, K. W. Murch, R. Naik, A. N. Korotkov, and I. Siddiqi, Nature (London) **490**, 77 (2012).
[19] S. J. Weber, A. Chantasri, J. Dressel, A. N. Jordan, K. W. Murch, and I. Siddiqi, Nature (London) **511**, 570 (2014).
[20] M. Field, C. G. Smith, M. Pepper, D. A. Ritchie, J. E. F. Frost, G. A. C. Jones, and D. G. Hasko, Phys. Rev. Lett. **70**, 1311 (1993).
[21] Z. Shi, C. B. Simmons, D. R. Ward, J. R. Prance, R. T. Mohr, T. S. Koh, J. K. Gamble, X. Wu, D. E. Savage, M. G. Lagally *et al.*, Phys. Rev. B **88**, 075416 (2013).
[22] G. Cao, H.-O. Li, T. Tu, L. Wang, C. Zhou, M. Xiao, G.-C. Guo, H.-W. Jiang, and G.-P. Guo, Nat. Commun. **4**, 1401 (2013).
[23] D. Kim, D. R. Ward, C. B. Simmons, J. K. Gamble, R. Blume-Kohout, E. Nielsen, D. E. Savage, M. G. Lagally, M. Friesen, S. N. Coppersmith, and M. A. Eriksson, Nat. Nanotechnol. **10**(3), 243 (2015).
[24] J. M. Elzerman, R. Hanson, J. S. Greidanus, L. H. Willems van Beveren, S. De Franceschi, L. M. K. Vandersypen, S. Tarucha, and L. P. Kouwenhoven, Phys. Rev. B **67**, 161308 (2003).
[25] J. R. Petta, A. C. Johnson, C. M. Marcus, M. P. Hanson, and A. C. Gossard, Phys. Rev. Lett. **93**, 186802 (2004).
[26] N. P. Oxtoby, H. M. Wiseman, and H.-B. Sun, Phys. Rev. B **74**, 045328 (2006).
[27] J. M. Elzerman, R. Hanson, L. H. Willems van Beveren, B. Witkamp, L. M. K. Vandersypen, and L. P. Kouwenhoven, Nature (London) **430**, 431 (2004).
[28] J. R. Petta, A. C. Johnson, J. M. Taylor, E. A. Laird, A. Yacoby, M. D. Lukin, C. M. Marcus, M. P. Hanson, and A. C. Gossard, Science **309**, 2180 (2005).
[29] D. Aasen, M. Hell, R. V. Mishmash, A. Higginbotham, J. Danon, M. Leijnse, T. S. Jespersen, J. A. Folk, C. M. Marcus, K. Flensberg *et al.*, Phys. Rev. X **6**, 031016 (2016).
[30] A. A. Clerk, Phys. Rev. Lett. **96**, 056801 (2006).
[31] I. L. Aleiner, N. S. Wingreen, and Y. Meir, Phys. Rev. Lett. **79**, 3740 (1997).
[32] S. A. Gurvitz, Phys. Rev. B **56**, 15215 (1997).
[33] D. V. Averin and E. V. Sukhorukov, Phys. Rev. Lett. **95**, 126803 (2005).
[34] R. Egger and H. Grabert, Phys. Rev. B **58**, 10761 (1998).
[35] C. L. Kane and M. P. A. Fisher, Phys. Rev. Lett. **68**, 1220 (1992).
[36] P. W. Anderson, Phys. Rev. Lett. **18**, 1049 (1967).
[37] K. D. Schotte and U. Schotte, Phys. Rev. **182**, 479 (1969).
[38] T. Giamarchi, *Quantum Physics in One Dimension* (Oxford University Press, Oxford, 2004).
[39] A. J. Leggett, S. Chakravarty, A. T. Dorsey, M. P. A. Fisher, A. Garg, and W. Zwerger, Rev. Mod. Phys. **59**, 1 (1987).
[40] U. Weiss, *Quantum Dissipative Systems* (World Scientific, Singapore, 2012).
[41] M. P. A. Fisher and L. I. Glazman, in *Mesoscopic Electron Transport*, edited by L. L. Sohn, L. P. Kouwenhoven, and G. Schön, NATO Advanced Study Institute (Springer, The Netherlands, 1997).
[42] C. L. Kane and M. P. A. Fisher, Phys. Rev. B **46**, 15233 (1992).
[43] L. S. Levitov and M. Reznikov, Phys. Rev. B **70**, 115305 (2004).
[44] D. Bagrets, Y. Utsumi, D. Golubev, and G. Schön, Fortschr. Phys. **54**, 917 (2006).
[45] A. Furusaki, Phys. Rev. B **57**, 7141 (1998).
[46] T. Li, P. Wang, H. Fu, L. Du, K. A. Schreiber, X. Mu, X. Liu, G. Sullivan, G. A. Csáthy, X. Lin, and R-R. Du, Phys. Rev. Lett. **115**, 136804 (2015).
[47] E. Levy, I. Sternfeld, M. Eshkol, M. Karpovski, B. Dwir, A. Rudra, E. Kapon, Y. Oreg, and A. Palevski, Phys. Rev. B **85**, 045315 (2012).
[48] H. Ishii, H. Kataura, H. Shiozawa, H. Yoshioka, H. Otsubo, Y. Takayama, T. Miyahara, S. Suzuki, Y. Achiba, M. Nakatake, T. Narimura, M. Higashiguchi, K. Shimada, H. Namatame, and M. Taniguchi, Nature (London) **426**, 540 (2003).